



Original article

Eight Zhes Decoction ameliorates the lipid dysfunction of nonalcoholic fatty liver disease using integrated lipidomics, network pharmacology and pharmacokinetics

Yuping Zhou^{a, b, c}, Ze Dai^{a, b}, Kaili Deng^{a, b}, Yubin Wang^b, Jiamin Ying^b, Donghui Chu^b, Jinyue Zhou^b, Chunlan Tang^{a, b, *}

^a The First Affiliated Hospital of Ningbo University, Ningbo, Zhejiang, 315020, China

^b School of Public Health, Health Science Center, Ningbo University, Ningbo, Zhejiang, 315211, China

^c Institute of Digestive Disease of Ningbo University, Ningbo, Zhejiang, 315020, China

ARTICLE INFO

Article history:

Received 8 February 2023

Received in revised form

19 April 2023

Accepted 21 May 2023

Available online 24 May 2023

Keywords:

Eight Zhes Decoction

Nonalcoholic fatty liver disease

Lipidomics

Network pharmacology

Pharmacokinetics

ABSTRACT

Nonalcoholic fatty liver disease (NAFLD) has developed into the most common chronic liver disease and can lead to liver cancer. Our laboratory previously developed a novel prescription for NAFLD, “Eight Zhes Decoction” (EZD), which has shown good curative effects in clinical practice. However, the pharmacodynamic material basis and mechanism have not yet been revealed. A strategy integrating lipidomics, network pharmacology and pharmacokinetics was used to reveal the active components and mechanisms of EZD against NAFLD. The histopathological results showed that EZD attenuated the degrees of collagen deposition and steatosis in the livers of nonalcoholic steatofibrosis model mice. Furthermore, glycerophospholipid metabolism, arachidonic acid metabolism, glycerolipid metabolism and linoleic acid metabolism with phospholipase A2 group IVA (PLA2G4A) and cytochrome P450 as the core targets and 12,13-*cis*-epoxyoctadecenoic acid, 12(*S*)-hydroxyeicosatetraenoic acid, leukotriene B4, prostaglandin E2, phosphatidylcholines (PCs) and triacylglycerols (TGs) as the main lipids were found to be involved in the treatment of NAFLD by EZD. Importantly, naringenin, artemetin, canadine, and bicuculline were identified as the active ingredients of EZD against NAFLD; in particular, naringenin reduces PC consumption by inhibiting the expression of PLA2G4A and thus promotes sufficient synthesis of very-low-density lipoprotein to transport excess TGs in the liver. This research provides valuable data and theoretical support for the application of EZD against NAFLD.

© 2023 The Authors. Published by Elsevier B.V. on behalf of Xi'an Jiaotong University. This is an open access article under the CC BY-NC-ND license (<http://creativecommons.org/licenses/by-nc-nd/4.0/>).

1. Introduction

Nonalcoholic fatty liver disease (NAFLD) is an acquired metabolic stress liver injury disease, and its pathogenesis is relevant to type 2 diabetes, obesity, hyperlipidemia, hypertension, and metabolic risk factors. Simple fatty liver disease, nonalcoholic steatohepatitis (NASH) and related cirrhosis are some of the different manifestations and pathological processes of NAFLD. In the absence of excessive alcohol intake or other chronic liver diseases, more than 5% of hepatocyte steatosis is considered diagnostic of NAFLD [1]. The global prevalence of NAFLD reached 29.8% in 2019 and will

continue to rise in the next few decades [2]. More importantly, NAFLD has evolved into the most common chronic liver disease worldwide over the past two decades and poses a serious clinical burden, economic burden and impact on patients' lives.

The causes of NAFLD mainly include insulin resistance, intestinal flora disorders, abnormal lipid metabolism, and mitochondrial dysfunction [3]. One of the core factors causing pathological effects is the accumulation of toxic lipid substances, which is mainly caused by abnormal metabolism [4]. These lipotoxic lipids include diacylglycerols (DGs) [5], ceramides (Cers) [6], lysophosphatidylcholines (LPCs) [7], and excessive cholesterols (Chos) [8], which contribute to the stress, injury and death of liver cells and thus further lead to liver fibrosis. Although these lipotoxic lipids that promote cellular damage and inflammatory responses have not been fully defined and their specific mechanisms have not been fully explored, reducing the accumulation of

Peer review under responsibility of Xi'an Jiaotong University.

* Corresponding author. The First Affiliated Hospital of Ningbo University, Ningbo, Zhejiang, 315020, China.

E-mail address: chunlant@163.com (C. Tang).

these lipids is a reliable method for preventing and controlling NAFLD.

Currently, the diagnosis and therapy of NAFLD is extremely limited. An effective method is to control a patient's weight to some extent because maintaining a body weight loss 10% can reduce the risk of liver fibrosis [9]. With the changing disease spectrum, many patients are now leaner [10,11]. The dysfunction of lipid metabolism in the liver as a result of nutritional imbalance leads to rapid and massive accumulation of triacylglycerols (TGs) in hepatocytes, resulting in the development of NAFLD. The drugs currently in clinical trials include vitamin E, pioglitazone, glucagon like peptide-1 agonists, peroxisome proliferator-activated receptor- γ agonists, and sodium-dependent glucose transporter 2 inhibitors, but their clinical use remains limited due to potential side effects and uncertainty regarding long-term efficacy and safety.

Traditional Chinese medicines (TCMs) have remarkable therapeutic effects on NAFLD. Yinchenhao decoction, Shenling Baizhu powder, Daibuhu decoction, Taohong Siwu decoction, Qianggan prescription and other TCM prescriptions can significantly reverse the liver pathological manifestations of NAFLD [12]. However, it is well known that the ingredients and targets of TCMs in most cases are quite complicated and difficult to identify. Lipidomics focuses on the holistic and systematic study of lipid changes *in vivo*, which coincides with the holistic view of TCMs. Therefore, this strategy is widely employed to clarify the mechanism of medicines in modern Chinese medicine. The key lipid molecules of Shenling Baizhu powder [13] and Dohongsamul-tang [14] in the treatment of NAFLD were preliminarily determined as potential therapeutic targets. Although lipidomics can reflect the changed lipids by TCMs, the specific ingredients that cause these changes and their upstream proteins remain unclear. Network pharmacology and pharmacokinetics have been widely used in TCMs because they reveal the effective ingredients, predict the potential targets of known compounds, and explain the mechanism.

Our research group developed a novel prescription denoted "Eight Zhes Decoction" (EZD) based on many years of practice in TCM clinical treatment of NAFLD, and this decoction has achieved good clinical efficacy against NAFLD [15]. However, the mechanism of EZD against NAFLD remains unknown and requires further study. Therefore, the present study used the nonalcoholic steatofibrosis (NASF) mouse model and combined the techniques of lipidomics, network pharmacology, and pharmacokinetics to study the active ingredients and mechanisms of EZD in NAFLD, and the results provide experimental support and a thorough understanding of the potential application of EZD against NAFLD in the clinic.

2. Materials and methods

2.1. Chemicals and reagents

Methionine-choline deficient feed (MCD) and control feed (MCS) were provided by Nantong Trophy Feed Technology Co., Ltd. (Nantong, China). The EZD consisted of eight genuine medicinal materials in Zhejiang Province, including *Curcuma Radix*, *Corydalis Rhizoma*, *Acteagelodes Macrocephalae Rhizoma*, *Fritillariae Thunbergii Bulbus*, *Paeoniae Radix Alba*, *Scrophulariae Radix*, *Chrysanthemi Flos*, and *Ophiopogonis Radix*, which were purchased from Ningbo Mingbei Chinese Pharmaceutical Co., Ltd. (Ningbo, China). The crude drugs were identified by Jun Bao from the First Affiliated Hospital of Ningbo University. The voucher specimens were deposited in the abovementioned hospital. The lipid standards were purchased from Sigma-Aldrich (St. Louis, MO, USA) or Avanti Polar Lipids (Alabaster, AL, USA). The reagents were all of high performance liquid chromatography-grade and included formic acid (FA) from Sigma-Aldrich; *tert*-butyl methyl ether

(MTBE), isopropanol (IPA), methanol (MeOH), and acetonitrile (ACN) from Merck (Darmstadt, Germany); ammonium formate (AmFA) and dichloromethane (CH_2Cl_2) from Thermo Fisher Scientific Inc. (Waltham, MA, USA); and carbon tetrachloride (CCl_4) from Sinopharm Chemical Reagent Shanghai Co., Ltd. (Shanghai, China). The primary antibodies were obtained from Boster Biotechnology and Proteintech (Wuhan, China), and horseradish peroxidase-conjugated secondary antibody was provided by Cell Signaling Technology (Boston, MA, USA). Fetal bovine serum (FBS), base medium, and penicillin-streptomycin solution (P/S) were purchased from Gibco Life Technologies (Grand Island, NE, USA). The high-fat cell additive (SYSJ-KJ006) was provided by Xi'an Kunchuang Corporation (Xi'an, China). The total TG assay kit was obtained from Nanjing Jiancheng Bioengineering Institute (Nanjing, China), and oil red O was provided by Beijing Solarbio Science & Technology Co., Ltd. (Beijing, China). Ultrapure water was obtained using a Milli-Q system (Millipore, Billerica, MA, USA).

2.2. Animals

C57BL/6J mice (24 ± 3 g) were obtained from Jiangsu Jicui Yaokang Biotechnology Co., Ltd. All animal experiments were approved by the Experimental Animal Ethics Committee of Ningbo University (Approval number: SYXK (Zhejiang) 2019-0005).

Three groups, namely normal group (N), NASF model group (6W), and EZD group (Z), were separated, and each group consisted of 8 mice. The NASF model mice were obtained by feeding an MCD diet and administering an intraperitoneal injection of 10% CCl_4 -olive oil solution (2 mL/kg) once a week for 6 weeks. The normal mice were fed the MCS diet. The EZD dose administered to the mice was converted from the dose used for clinical administration. The daily dose of EZD for human adults is based on the following amounts of the crude drugs: *Curcuma Radix* (12 g), *Fritillariae Thunbergii Bulbus* (12 g), *Chrysanthemi Flos* (12 g), *Acteagelodes Macrocephalae Rhizoma* (15 g), *Paeoniae Radix Alba* (12 g), *Scrophulariae Radix* (12 g), *Ophiopogonis Radix* (12 g), and *Corydalis Rhizoma* (9 g). The total mass of the crude drugs used in the clinic is 96 g, which equates to a dose of 1.37 (96/70) g/kg body weight. The daily EZD dose for mice was calculated by converting the body surface area of human adults (70 kg) to that of mice as follows: $1.37 \text{ g/kg} \times 10 = 13.7 \text{ g/kg} \approx 14 \text{ g/kg}$ (20 mL/kg). EZD was administered to the mice once a day for 4 weeks beginning from the third week of model establishment. The normal and model groups were administered an equal dose (20 mL/kg) of saline by gavage. After 6 weeks of feeding, the animals were fasted for 12 h, and liver tissues were collected after anesthesia.

2.3. Cell experiment

L02 cells were cultured in 1,640 medium containing 10% FBS and 1% P/S at 37 °C and 5% carbon dioxide. The cells were washed twice with phosphate buffered saline solution and suspended in complete medium containing sodium palmitate (250 μM) and sodium oleate (500 μM) after reaching 50%–60% confluence. Stock solutions of naringenin, artemetin, canadine, and bicuculline were prepared with dimethylsulfoxide (DMSO) and then added to the cell supernatants. The final concentration of DMSO in all the groups was 0.1%. After 48 h of intervention, oil red O staining was carried out, and 3% Triton was added to the cells for the extraction of total intracellular triglycerides for later analysis.

2.4. Sample preparation and extraction

2.4.1. Standard stock solutions

Standard stock solutions (1 mg/mL) of canadine, naringenin, bicuculline, and artemetin were prepared in MeOH and then diluted

to the following concentrations for the calibration curve: canadine (16, 32, 64, 128, and 256 ng/mL), artemetin (16, 32, 64, 128, and 256 ng/mL), naringenin (1, 2, 3, 4, and 5 ng/mL), and bicuculine (4, 8, 16, 32, and 64 ng/mL).

2.4.2. EZD

The decoction was prepared using the same protocol as that used for the conventional Chinese medicine decoction. The herbal crude slices were mixed, soaked in cold water for 30 min (2–3 cm above the height of the drug surface) and boiled for 10 min under high heat and 30 min under low heat, and the liquid was then poured into a reagent bottle. The dregs of the decoction were then added to cold water (2–3 cm above the height of the drug surface) and decocted as described before under high and low heat, and the liquid was then poured into a reagent bottle. The two decoctions were mixed together and concentrated to a concentration of 0.70 g/mL by a rotary evaporator. The mice were orally administered the resulting drug, simulating the process of clinical patient use, without freezing, drying or sterilization. In addition, EZD (200 mg/mL) in MeOH:H₂O (1:1, V/V) solution was prepared to carry out the quantitative analysis.

2.4.3. Lipid analysis

The liver sample was weighed (20 mg) and homogenized with steel balls for 20 s. One milliliter of MTBE:MeOH mixed solvent (3:1, V/V) including internal standards was then added and stirred for 15 min. Subsequently, H₂O (200 µL) was added, and the mixture was stirred again for 1 min. The upper layer (200 µL) was obtained by centrifugation, and further concentrated and dissolved with 200 µL of ACN:IPA (10:90, V/V) solution for analysis.

2.4.4. Absorbed ingredient analysis

Forty milligrams of liver sample was weighed and homogenized with a steel ball for 20 s. MeOH (1 mL) was added to extract compounds. The sample was mixed for 10 min and centrifuged to obtain the upper layer for vacuum drying. Two hundred microliters of MeOH:H₂O (1:1, V/V) solution was used to reconstitute the sample for analysis.

2.5. Histologic assessment

Paraffin sections of liver tissue were prepared for Masson staining for the observation of tissue collagen hyperplasia. Liver tissue was frozen and stained with oil red O for the observation of fatty deposition.

2.6. Lipid and active ingredient detection

Lipid detection: A SCIEX QTRAP liquid chromatography-tandem mass spectrometry system (Shanghai, China) and a C₃₀ column (2.1 mm × 100 mm, 2.6 µm) at 45 °C were employed to separate and detect the lipids (Thermo Scientific Inc., San Jose, CA, USA). The solvent system included ACN:H₂O (60:40, V/V; A) and ACN:IPA (10:90, V:V; B), both with 0.1% FA and 10 mM AmFA. The flow rate was 0.35 mL/min. Gradient elution was used as follows: 20%–30% B at 0–2 min, 30%–60% B at 2–4 min, 60%–85% B at 4–9 min, 85%–90% B at 9–14 min, 90%–95% B at 14–15.5 min, 95% B at 15.5–17.3 min, and 20% B at 17.3–20 min. The injection volume was set to 2 µL. The optimized mass spectrometry conditions were as follows: linear ion trap and triple quadrupole scan types; ion source temperature, 500 °C; collision gas, nitrogen (5 psi); curtain gas, 35 psi; ion source gas 1 and 2, 45 and 55 psi; and ion spray voltages, 5,500 V and –4,500 V.

Active ingredient detection: A Waters Xevo G2-XS quadrupole time of flight mass spectrometry system and Acquity UPLC HSS T₃

column (2.1 mm × 150 mm, 1.7 µm) at 40 °C were employed (Milford, MA, USA). The mobile phases were 0.1% FA:H₂O (V/V) (A) and ACN (B). Gradient elution was used as follows: 20% B at 0–3 min, 20%–95% B at 3–9 min, 95% B at 9–12 min, and 95%–20% B at 12.1–14 min. The flow rate and injection volume were 0.3 mL/min and 5 µL, respectively. The optimized MS conditions were used: capillary voltages, 2.5 kV (negative) and 3 kV (positive); acquisition range, 100–1,200 *m/z*; scan time, 0.1 s; nebulizer and auxiliary gas, nitrogen (400 °C and 1,000 L/h); and collision energy, 20 or 35 eV.

2.7. Network construction

The TCMSD database was adopted to find the compounds of EZD based on the criteria with oral bioavailability ≥30% and drug-likeness ≥0.18 [16]. To avoid missing active ingredients, compounds reported in the literature that did not satisfy the standards but exhibited high activity and/or were found at a high content were also selected for further study. The structures of all screened compounds transformed into SDF or canonical SMILES formats were imported into the Stitch [17], Swiss Target Prediction (STP) [18], PharmMapper [19], and Similarity Ensemble Approach (SEA) [20] servers to predict targets in *Homo sapiens*. Furthermore, the GeneCards database was used to obtain NAFLD-related targets [21]. Two sets of targets were matched, and the mutual targets were collected. The DAVID database was adopted for further Kyoto Encyclopedia of Genes and Genomes (KEGG) pathway and Gene Ontology (GO) enrichment analyses with *Homo sapiens* as the condition [22]. The compound-target (C-T) network and compound-reaction-enzyme-gene (CREG) network were built and visualized using Cytoscape 3.9.1 [23].

2.8. Molecular docking

The structures of proteins and ligands from the Protein Data Bank [24] and PubChem [25] databases were introduced into PyMOL (Version 2.0 Schrödinger, LLC) to remove water molecules. Docking and the affinity calculation between the ligand and protein were conducted using AutoDockTools-1.5.6 [26].

2.9. Western blotting

Cells (1 × 10⁶) were collected from different treatment groups, and 200 µL of radioimmunoprecipitation assay solution was added for 30 min at 4 °C for cell lysis. An ultrasonic crushing instrument was then used to administer ultrasound waves for 10 s at 40 W at intervals of 50 s for a total of 5 cycles. The electrophoresis conditions were maintained at 80 V for 0.5 h followed by 1 h at 120 V, and the transmembrane condition was maintained at 400 mA for 70 min. The membrane was then incubated with 5% skim milk for 2 h with primary antibody overnight and with secondary antibody the next day. The membrane was cleaned with Tris buffer solution plus Tween after each incubation. The relative protein expression content was detected using the enhanced chemiluminescence luminescence method, and the image was analyzed with ImageJ (6.0) software [27].

2.10. Statistical analysis

Principal component analysis (PCA) and orthogonal partial least squares-discriminant analysis (OPLS-DA) were carried out with R (www.r-project.org). SPSS 16.0 software (Chicago, IL, USA) was used for *t* tests or one-way analysis of variance. *P* < 0.05 was considered to indicate significance.

3. Results

3.1. EZD alleviated the histopathological disorder

A high degree of steatosis was observed in liver tissue of the NASF model mice by oil red O staining, and the cytoplasm was full of vacuoles of lipid droplets. Quantification of the oil red O-stained area was accomplished using the lipid droplet area. The lipid droplet area was markedly increased in the NASF model group, but the degree of steatosis and the lipid droplet area of the EZD intervention group were significantly decreased ($P < 0.01$). Masson staining can be used to visualize the distribution of collagen fibers and muscle fibers, and the proportion of the collagen fiber content can be analyzed semiquantitatively by calculating the collagen volume fraction (CVF). In the NASF model group, the collagen deposition of liver tissue was markedly increased, collagen fibers were found to form a filamentous or even coarse cord-like distribution around the sinusium, the hepatic lobule structure was disorganized, and fibrous tissue hyperplasia was also observed. EZD attenuated the degree of collagen deposition. The CVF values were significantly increased ($P < 0.01$) and decreased ($P < 0.05$) by NASF and EZD intervention, respectively. These results demonstrated that EZD can effectively alleviate the degree of NASF (Fig. 1).

3.2. Lipid profiles in liver tissue of EZD-treated NASF model mice

To further identify which lipid biomarkers are responsible for the effect of EZD against NAFLD, lipid profiling was performed. Prior to disposing the sample data, the quality control (QC) samples were subjected to Pearson correlation analysis. The correlation coefficient r was >0.9973 , which indicated high stability and repeatability. The representative total ion chromatogram of the QC sample and Pearson correlation analysis are presented in Figs. S1–S3. Thirty-two types of lipids and 1,321 lipids were identified in the livers of the normal, NASF model and EZD groups, and these included 291 TGs, 231 phosphatidylethanolamines (PEs), 134 phosphatidylcholines (PCs), and 99 DGs, etc. The total contents of LPCs, PCs, lysophosphatidylethanolamines (LPEs), TGs, Chos, sphingomyelins (SMs), coenzyme Qs (CoQs), PEs, DGs, phosphatidylserines (PSs), Cers, bile acids (Bas), lysophosphatidylinositols (LPIs), lysophosphatidylglycerols (LPGs), hexosylceramides (HexCers), lysophosphatidylserines (LPSs), bis (monoacylglycero)phosphates (BMPs), cholesteryl esters (CEs), lysophosphatidic acids (LPAs), eicosanoids, and sitosterol esters were significantly different between the normal group and the NASF model group ($P < 0.05$). In addition, the contents of Bas, Chos, DGs, eicosanoids and TGs were markedly different between the EZD group and the NASF model

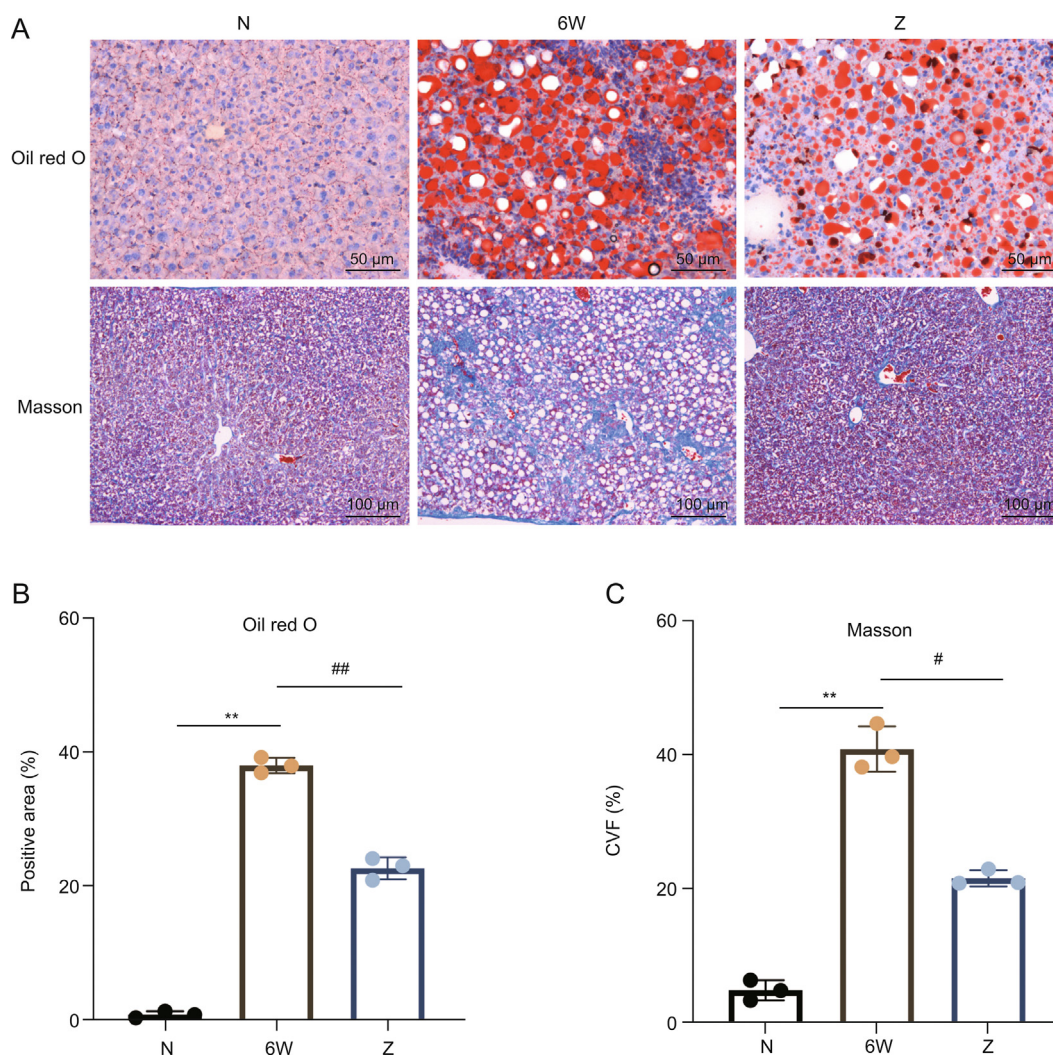


Fig. 1. Effect of Eight Zhes Decoction (EZD) on liver tissues of nonalcoholic steatofibrosis (NASF) model mice. (A) Histopathological changes in liver tissues of the normal (N), model (6W) and EZD (Z) groups detected by oil red O and Masson staining. (B) Lipid droplet area (positive area) ratio of liver tissues. (C) Collagen volume fraction (CVF) values of liver tissue. ** $P < 0.01$ vs. the normal group; # $P < 0.05$ and ## $P < 0.01$ vs. the model group.

group ($P < 0.05$), suggesting that significant lipid changes were induced by NASF model establishment and by the EZD therapy (Fig. 2A). Furthermore, PCA was carried out to observe the trends and show the differences between groups (Fig. 2B). A significant variation was obtained between the normal group and the NASF model group. Supplementation with EZD returned the lipid profile to normal to some extent, indicating that EZD can effectively relieve NASF in mice.

Then, OPLS-DA, a supervised pattern recognition method, was performed to find potential lipid markers for NAFLD and EZD treatment and further verify the separation of the lipid profiles between groups. The three main parameters of R^2X , R^2Y and Q^2 obtained by permutation test model validation were all greater than 0.5 (Figs. S4 and S5), suggesting the feasibility of the OPLS-DA model. The score plots showed obvious separation among the groups (Figs. 3A and B). The parameters used for screening the candidate lipid biomarkers were set as follows: $VIP \geq 1$, $P < 0.05$ and fold change ≥ 2 . Finally, 677 lipids with levels significantly affected by NASF were identified (Fig. 3C). Among them, 488 were upregulated, and these mainly belonged to 8 major lipid classes, which included free fatty acids (FFAs), TGs, Cers, DGs, CEs, PSs, BMPs, and phosphatidylglycerol (PGs), whereas the significantly downregulated 189 lipids included eicosanoid, LPE, LPC, phosphatidylinositol (PI) and PC classes. Similarly, 177 lipids were significantly affected by EZD (Fig. 3D), and these included 146 markedly downregulated lipids and 31 upregulated lipids. Based on the Venn diagram, 118 lipids (Table S1) showed significant differences between the normal and NASF model groups and the NASF model and EZD groups, and the changes in some lipids are shown in a heatmap (Fig. 3E). Among them, 19 lipids, namely, ursodeoxycholic acid, taurochenodeoxycholic acid, LPI(18:0/0:0), LPE(17:0/0:0), PC(18:1_22:5), PI(16:1_18:1), LPC(19:1/0:0), LPI(17:0), LPE(18:2/

0:0), LPI(19:0), PC(22:6_22:6), LPC(0:0/19:0), carnitine C6-OH, carnitine C5:1, carnitine C10:2, LPC(0:0/17:0), LPC(16:1/0:0), LPE(17:1/0:0), and LPE(20:2/0:0), were markedly decreased in the NASF model group but exhibited marked recovery after EZD therapy. The other 99 lipids were significantly increased in the NASF model group and recovered after EZD treatment.

3.3. Candidate compounds and target analysis

A total of 136 candidate compounds of EZD (Table S2) were collected, and these comprised 11 compounds from *Atractylodis Macrocephalae Rhizoma*, 22 from *Paeoniae Radix Alba*, 17 from *Fritillariae Thunbergii Bulb*, 12 from *Scrophulariae Radix*, 24 from *Chrysanthemi Flos*, 14 from *Ophiopogonis Radix*, 15 from *Curcumae Radix*, and 24 from *Corydalis Rhizoma*. Among these compounds, kaempferol and catechin are present in both *Paeoniae Radix Alba* and *Chrysanthemi Flos*, and naringenin is present in both *Chrysanthemi Flos* and *Curcumae Radix*. The targets of these compounds were predicted using the SEA, STP, Stitch, and PharmMapper servers. Finally, 281 disease-related targets of EZD were obtained (Table S3).

3.4. Joint pathway analysis of network pharmacology and lipidomics

A joint pathway analysis was conducted to explore the mechanism of EZD against NAFLD based on 118 differential lipids (Table S1) and 281 targets (Table S3) using MetaboAnalyst. The results showed that linoleic acid metabolism, arachidonic acid metabolism, glycerolipid metabolism and glycerophospholipid metabolism were highly enriched (Fig. 4A). Furthermore, a CREG network was constructed based on the changed lipids (Fig. S6). The above four pathways were

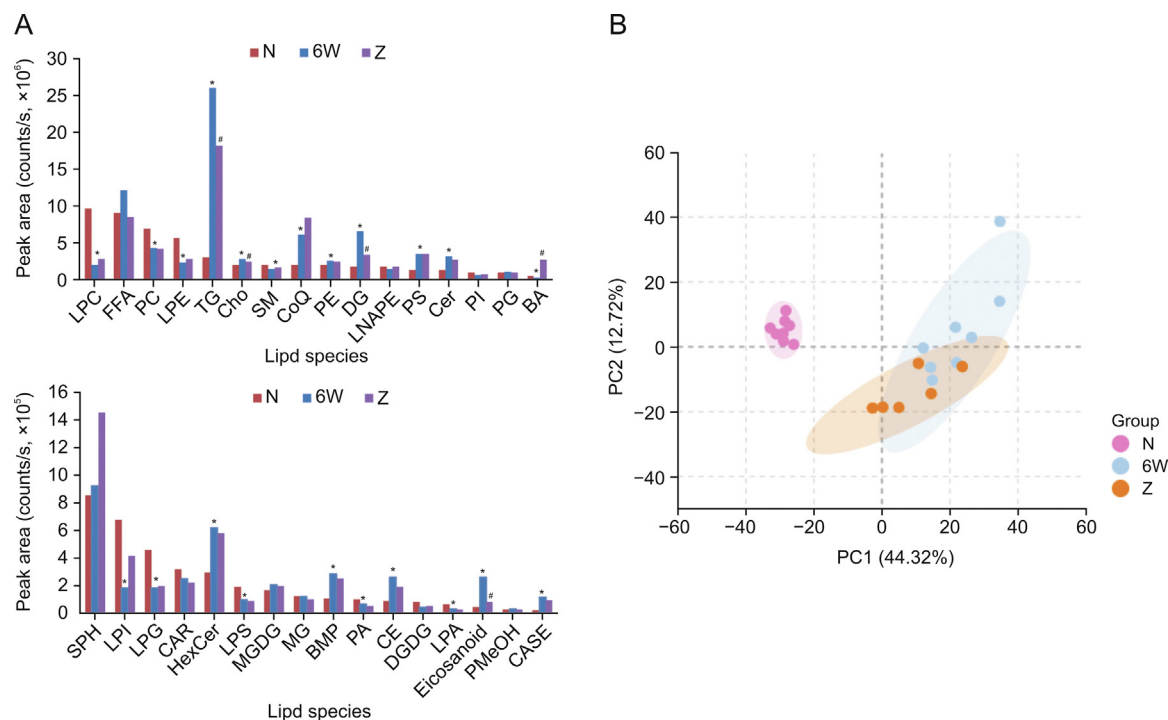


Fig. 2. Lipidomics analysis of liver tissues. (A) Intensity of different lipid species in the liver of the normal (N), model (6W) and Eight Zhes Decoction (EZD) (Z) groups ($n = 8$). * and # indicate statistically significant differences between the N and 6W groups and the 6W and Z groups ($P < 0.05$), respectively. (B) Principal component analysis (PCA) score plot of the hepatic lipid profiles of the normal, model and EZD groups. LPC: lysophosphatidylcholine; FFA: free fatty acid; PC: phosphatidylcholine; LPE: lysophosphatidylethanolamine; TG: triacylglycerol; Cho: cholesterol; SM: sphingomyelin; CoQ: coenzyme Q; PE: phosphatidylethanolamine; DG: diacylglycerol; LNAPE: *N*-acyl-lysophosphatidylethanolamine; PS: phosphatidylserine; Cer: ceramide; PI: phosphatidylinositol; PG: phosphatidylglycerol; BA: bile acid; SPH: sphingosine; LPI: lysophosphatidylinositol; LPG: lysophosphatidylglycerol; CAR: carnitine; HexCer: hexosylceramide; LPS: lysophosphatidylserine; MGDG: monogalactosyldiacylglycerol; MG: monoacylglycerol; BMP: bis (monoacylglycerol) phosphates; PA: phosphatidic acid; CE: cholesteryl ester; DGDG: digalactosyldiacylglycerol; LPA: lysophosphatidic acid, PMeOH: phosphatidylmethanol; CASE: sitosterol ester.

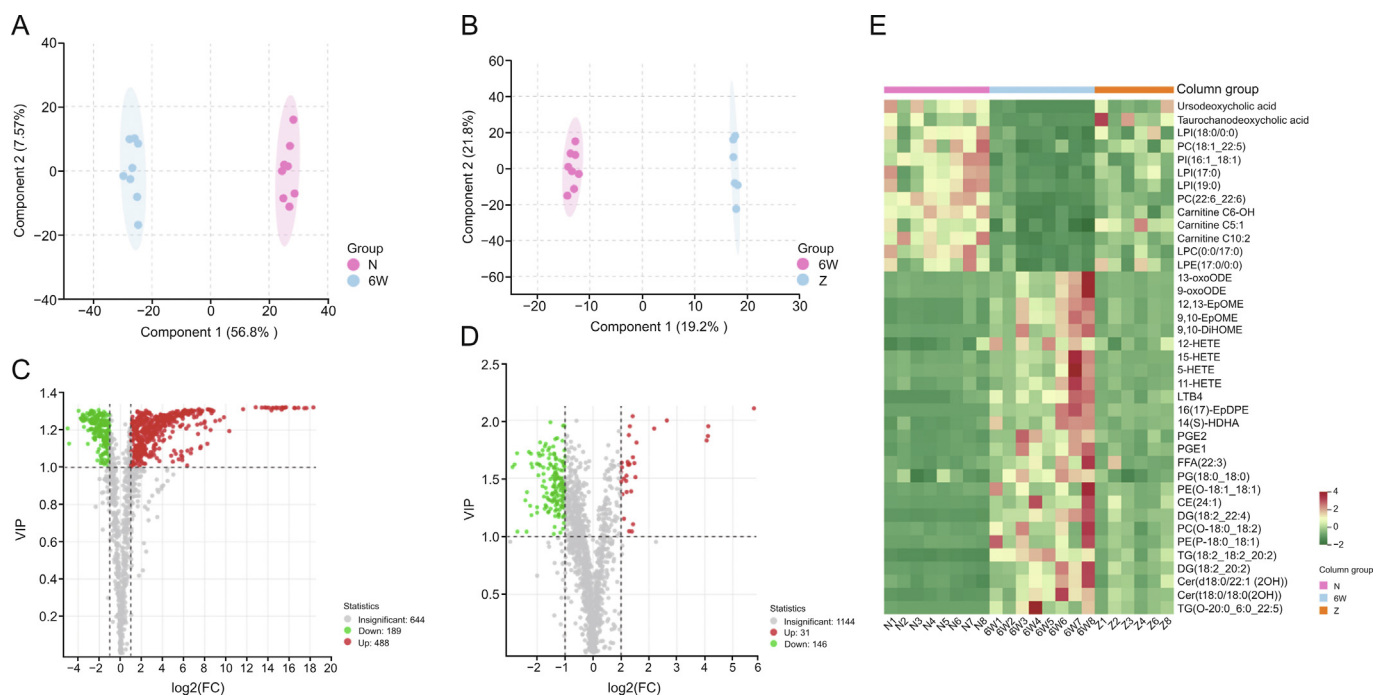


Fig. 3. Screening of significantly differential lipids. Orthogonal partial least squares-discriminant analysis (OPLS-DA) score plots and volcano plots of (A, C) the normal (N) versus model group (6W) and (B, D) the 6W versus Eight Zhes Decoction (EZD) (Z) group. (E) Heatmap analysis of some significantly differential lipids in the normal, model, and EZD groups. LPI: lysophosphatidylinositol; PC: phosphatidylcholine; PI: phosphatidylinositol; LPC: lysophosphatidylcholine; LPE: lysophosphatidylethanolamine; 13-oxoODE: 13-keto-9,11-octadecadienoic acid; 9-oxoODE: 9-keto-10E, 12Z-octadecadienoic acid; 12,13-EpOME: 12,13-cis-epoxyoctadecenoic acid; 9,10-EpOME: 9,10-epoxyoctadecenoic acid; DiHOME: dihydroxyoctadec-12-enoic acid; 12-HETE: 12(S)-hydroxyeicosatetraenoic acid; 15-HETE: 15(S)-hydroxyeicosatetraenoic acid; 5-HETE: 5-hydroxyeicosatetraenoic acid; 11-HETE: 11-hydroxyeicosatetraenoic acid; LTB4: leukotriene B4; PGE2: prostaglandin E2; PGE1: prostaglandin E1; FFA: free fatty acid; PG: phosphatidylglycerol; PE: phosphatidylethanolamine; CE: cholesteryl ester; DG: diacylglycerol; TG: triacylglycerol.

also highly enriched. By matching the enriched targets of four pathways in MetaboAnalyst with the genes in CREG network, 10 targets, namely, phospholipase A2 group IIA (*PLA2G2A*), cytochrome P450 family 2 subfamily C member 8 (*CYP2C8*), cytochrome P450 family 3 subfamily A member 4 (*CYP3A4*), cytochrome P450 family 2 subfamily C member 9 (*CYP2C9*), cytochrome P450 family 1 subfamily A member 2 (*CYP1A2*), phospholipase A2 group IVA (*PLA2G4A*), carboxyl ester lipase (*CEL*), diacylglycerol *O*-acyltransferase 1 (*DGAT1*), acetylcholinesterase (*ACHE*), and arachidonate 12-lipoxygenase (*ALOX12*), were considered core targets, and the metabolites 12,13-cis-epoxyoctadecenoic acid (12,13-EpOME), PCs, DGs, 5-hydroxyeicosatetraenoic acid (5-HETE), TGs, LPCs, 9,10-epoxyoctadecenoic acid (9,10-EpOME), prostaglandin E2 (PGE2), 12(S)-hydroxyeicosatetraenoic acid (12-HETE), leukotriene B4 (LTB4), 15(S)-hydroxyeicosatetraenoic acid (15-HETE), and PEs were identified as key metabolites (Table 1). The significant changes in lipids are presented in Fig. 4B. A schematic of the disturbed lipid pathways related to NAFLD and EZD treatment is shown in Fig. 4C. Furthermore, a C-T network was constructed (Fig. 4D). Among the 20 compounds, acetin, hesperetin, naringenin, triflex OBP, catechin, apigenin, and quercetin exhibited a relatively high number of connections with degree >4, diosmetin, chrysoeriol, luteolin, isorhamnetin, artemetin, ruscogenin exhibited a relatively high number of connections with degree = 3, and eriodictyol, cyaniding, kaempferol, picropodophyllin, canadine, bicuculline, and curcumin exhibited a relatively high number of connections with degree = 2; thus, these compounds might be the active substances of EZD against NAFLD.

3.5. Detection of EZD ingredients in EZD and liver tissue

The absorbed ingredients of EZD in liver tissue were detected. Among 20 candidate compounds, 4 compounds, bicuculline,

canadine, artemetin, and naringenin were detected in the liver tissue of the EZD group but not in that of the normal and NASF model groups by accurate mass and fragment ions compared with standard compounds. The extracted ion chromatograms and MS² spectra of the four ingredients are shown in Fig. 5, and detailed information is listed in Table 2. Furthermore, given the interbatch variability in the concentrations of active ingredients, a quantitative analysis of the main active ingredients, including canadine, naringenin, bicuculline and artemetin, was carried out. The following regression equations were obtained: $y = 111x + 901$ (canadine, $r^2 > 0.99$), $y = 31x - 475$ (artemetin, $r^2 > 0.99$), $y = 18x - 28$ (bicuculline, $r^2 > 0.99$), and $y = 41x - 21$ (naringenin, $r^2 > 0.99$). EZD (200 mg/mL) was prepared for quantitative analysis. The contents of canadine, artemetin and naringenin in EZD were 132 ng/mL, 80 ng/mL and 2 ng/mL, respectively. Interestingly, bicuculline was not detected in EZD at a concentration of 4 g/mL under the analysis conditions. However, this compound was detected in the liver of the EZD group at a concentration of approximately 15 ng/mL. Therefore, we hypothesize that bicuculline may be metabolized from other ingredients and accumulate in the liver.

3.6. Molecular docking

Four compounds (naringenin, artemetin, canadine and bicuculline) screened from the C-T network and identified by ingredient detection were docked with their corresponding key targets (*PLA2G2A*, *CYP2C8*, *CYP3A4*, *CYP2C9*, *CYP1A2*, and *ALOX12*) selected from MetaboAnalyst and MetScape analysis to evaluate their potential interactions. All of the docking scores were less than -5, and the main interactions among these ligands and proteins were hydrogen-bonding interactions (Table 3), which indicated that the proteins had good binding activity with active ingredients (Figs.

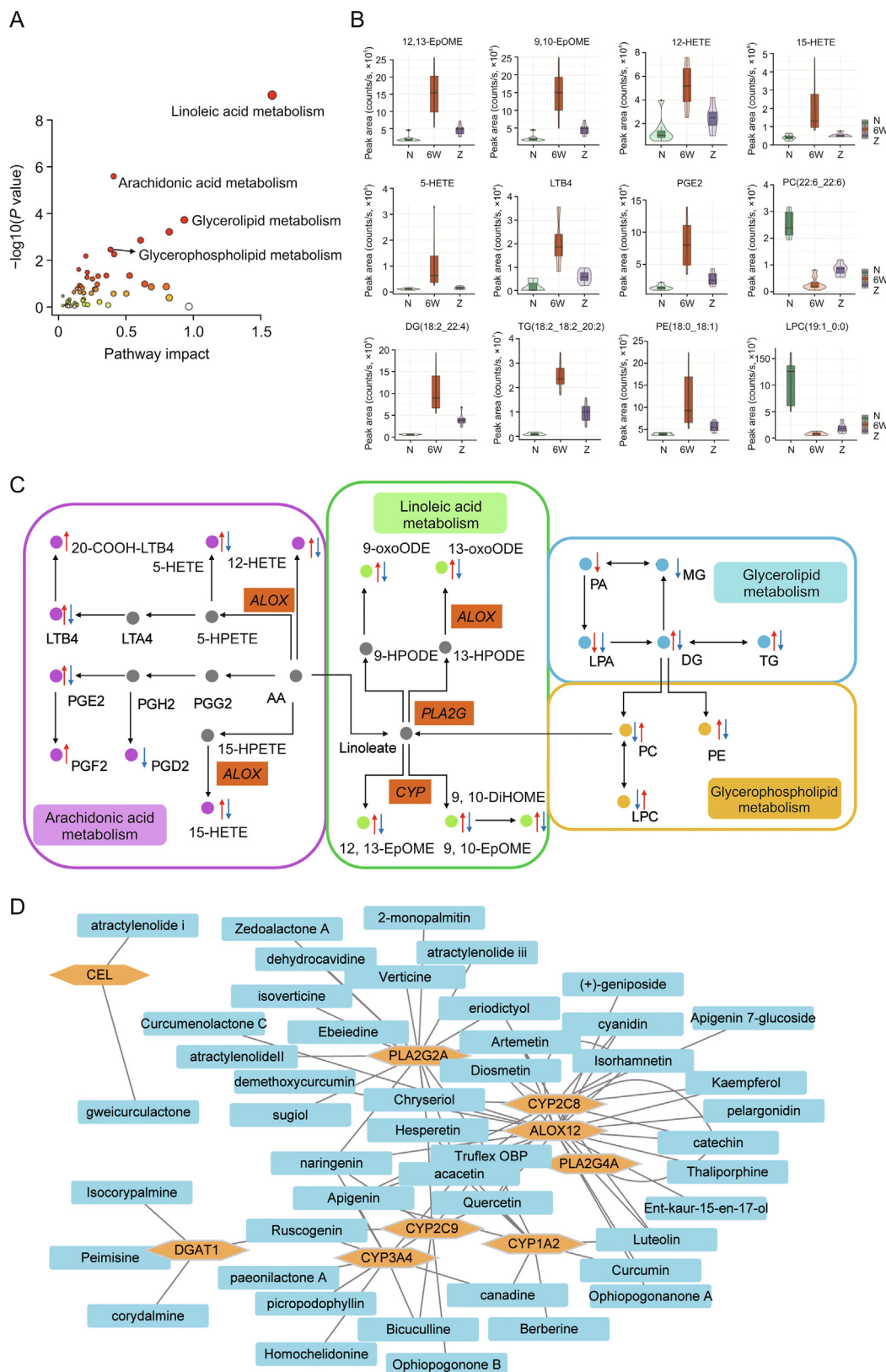


Fig. 4. Analysis of the main lipids, pathways and core targets. (A) Enrichment plot of pathways. (B) Intensity of the main lipid biomarkers among the three groups. (C) Schematic diagram of the disturbed lipid pathways related to nonalcoholic fatty liver disease and Eight Zhes Decoction (EZD) treatment. (D) Compound-target (C–T) network of ingredients and targets. LPC: lysophosphatidylcholine; PC: phosphatidylcholine; TG: triacylglycerol; PE: phosphatidylethanolamine; DG: diacylglycerol; MG: monoacylglycerol; PA: phosphatidic acid; LPA: lysophosphatidic acid; LTB4: leukotriene B4; HETE: hydroxyeicosatetraenoic acid; LTA4: leukotriene A4; HPETE: hydroperoxyeicosatetraenoic acid; PGE2: prostaglandin E2; PGH2: prostaglandin H2; PGG2: prostaglandin G2; PGF2: prostaglandin F2; PGD2: prostaglandin D2; 13-oxoODE: 13-keto-9,11-octadecadienoic acid; 9-oxoODE: 9-keto-10E, 12Z-octadecadienoic acid; HPODE: hydroperoxyoctadeca-9,12-dienoic acid; AA: arachidonic acid; EpOME: epoxy-octadecenoic acid; DiHOME: dihydroxyoctadec-12-enoic acid.

Table 1
Key pathways, targets and metabolites of Eight Zhes Decoction (EZD) against nonalcoholic fatty liver disease.

| Main pathway | Core targets | Key metabolites |
|--------------------------------|---|--|
| Linoleic acid metabolism | <i>PLA2G2A, CYP2C8, CYP3A4, CYP2C9, CYP1A2, PLA2G4A</i> | 12,13- <i>cis</i> -epoxyoctadecenoic acid, 9,10-epoxyoctadecenoic acid, phosphatidylcholine |
| Arachidonic acid metabolism | <i>PLA2G2A, CYP2C8, ALOX12, CYP2C9, PLA2G4A</i> | phosphatidylcholine, 12(<i>S</i>)-hydroxyeicosatetraenoic acid, 15(<i>S</i>)-hydroxyeicosatetraenoic acid, 5(<i>S</i>)-hydroxyeicosatetraenoic acid, leukotriene B ₄ , prostaglandin E ₂ |
| Glycerolipid metabolism | <i>CEL, DGAT1</i> | 1,2-diacyl- <i>sn</i> -glycerol, triglyceride |
| Glycerophospholipid metabolism | <i>PLA2G2A, ACHE</i> | 1-acyl- <i>sn</i> -glycero-3-phosphocholine, phosphatidylcholine, 1,2-diacyl- <i>sn</i> -glycerol, phosphatidylethanolamine |

6A–K). Furthermore, the active ingredient-metabolite-target-pathway network of EZD against NAFLD was constructed (Fig. 6L).

3.7. Validation of the effects of active ingredients against NAFLD and targets

To further identify the four active ingredients that play a role against NAFLD and verify the candidate targets that interact with active ingredients, L02 cells were induced to acquire a high-fat phenotype to establish a high-fat cell model. Oil red O staining showed that naringenin, artemetin, and bicuculline significantly reduced the content of total TGs and the lipid droplet area ratio, indicating that these compounds reversed intracellular triglyceride accumulation in the high-fat model group, and canadine had a similar, albeit not significant, effect (Figs. 7A–C). Naringenin reduced the protein expression levels of *PLA2G4A*, *ACHE*, and *DGAT1* in hepatocytes, and canadine significantly inhibited the expression of *ACHE*. In addition, the expression of *CYP2C8* was decreased significantly in all treatment groups (Fig. 7D).

4. Discussion

The continuing increase in the incidence of NAFLD seriously influences people's health and imposes a growing clinical and economic burden on many countries. However, there has been a lack of consensus on drugs to treat NAFLD until now. In recent years, many TCMs have been shown to prevent and treat NAFLD. EZD is a clinically used Chinese herbal prescription that has been used in our hospital for many years without clinical adverse events, and only a small minority of patients exhibit mild gastrointestinal reactions [15]. Our clinical practice has also confirmed that EZD has good therapeutic effects in NAFLD patients [15]. This study also showed that EZD can reverse hepatic steatosis and fibrosis in NASF model mice, reinforcing our previous observation that EZD can improve NAFLD. However, the specific mechanism and the active ingredients remain unclear. The present study combined lipidomics, network pharmacology and pharmacokinetics strategies to further explore the bioactive ingredients and therapeutic mechanism of EZD in NAFLD.

Metabolic disorders and toxic lipid hoarding products are considered the core links in the development of NAFLD [6]. Therefore, lipidomics is often used to link lipid disorders with pathological changes in the liver in NAFLD. It has been reported that Babao Dan [28], Shenling Baizhu San [13], saikosaponins A and D [29], Dohongsamul-tang [14], Highland Barley β Glucan [30] and other Chinese herbs can improve the pathological manifestations and change some types of liver lipids in NAFLD. Therefore, lipidomics and network pharmacology approaches were applied to depict the lipid profile and mechanism of EZD against NAFLD in our study. The lipid profiles were significantly disturbed in NASF model mice and recovered after EZD intervention. Network pharmacology showed that EZD ingredients act on multiple targets of NAFLD. By

integrating the lipidomics pathway and the target pathways predicted by network pharmacology, glycerophospholipid metabolism, arachidonic acid metabolism, glycerolipid metabolism and linoleic acid metabolism were found to be significantly changed by NAFLD development and EZD intervention. The key metabolites are 12,13-EpOME, PCs, DGs, TGs, LPCs, 9,10-EpOME, 12-HETE, LTB₄, 5-HETE, PGE₂, 15-HETE, and PEs, and the core targets are *PLA2G2A, CYP2C8, CYP3A4, CYP2C9, CYP1A2, PLA2G4A, CEL, DGAT1, ACHE*, and *ALOX12*.

The hepatic accumulation of TGs has been considered the beginning of the development of NAFLD. Several studies have revealed elevated TG levels in patients with NAFLD [31,32]. Hence, several studies on the use of TGs as biomarkers for NAFLD have been performed [33,34]. The present study also showed an increase in most TGs in the liver tissue of NASF mice, and EZD effectively reduced the accumulation of TGs in liver tissue to alleviate NAFLD. Glycerophospholipids can also be targets of protein signaling molecules and play an essential role in the physiological process of cells. Glycerophospholipids include PS, PC, PI, PE, and PG. PC is known as the only phospholipid that affects lipoprotein assembly and secretion. After synthesis in the liver, TGs bond with lipoproteins and phospholipids to generate very-low-density lipoprotein (VLDL) and are further transported to the blood. Therefore, VLDL secretion in blood is highly regulated by the level of PC, and dysfunction of VLDL secretion results in the accumulation of liver TGs [35]. Our results demonstrated a decreased PC level in the livers of NASF mice. When the PC content is insufficient, sufficient VLDL cannot be synthesized to transport TG in the liver, resulting in excessive liver lipid deposition. However, EZD restored the level of PCs, suggesting that EZD plays a role by regulating the dynamic balance between PC and TG in the liver.

PC can be converted to arachidonic acid (AA) by phospholipase A₂ (*PLA2*), which is widespread in the human body. AA can be further oxidized to generate oxidized AA by lipoxygenases, cyclooxygenases and CYP450. Puri et al. studied the circulating levels of oxidative AA in healthy, steatotic and NASH patients and found that the levels of lipoxygenase (*LOX*) metabolites, including 15-HETE, 8(*S*)-hydroxyeicosatetraenoic acid (8-HETE) and 5-HETE, were elevated [36]. Barr et al. noted increases in a series of metabolites (HETEs) in NASH patients [37]. Our results also showed that 5-HETE, 12-HETE and 15-HETE were significantly increased in the livers of NASF model mice, found that EZD intervention mitigated this disorder, and identified *ALOX12* as the core target of EZD in NAFLD. Another important *LOX* metabolite is LTB₄, a proinflammatory cytokine and a hallmark of liver inflammation [38]. Liu et al. also reported that LTB₄/LTB₄ receptor 1 (*Ltb4r1*) promotes hepatocyte adipogenesis through activation of *PKA-IRE1α-XBP1s*. Therefore, *Ltb4r1* might be a potential target in NAFLD [39]. PGE₂, a cyclooxygenase (*COX*) metabolite of AA, is significantly involved in abnormal lipid metabolism by inhibiting fatty acid oxidation, lipolysis and VLDL synthesis during liver lipid

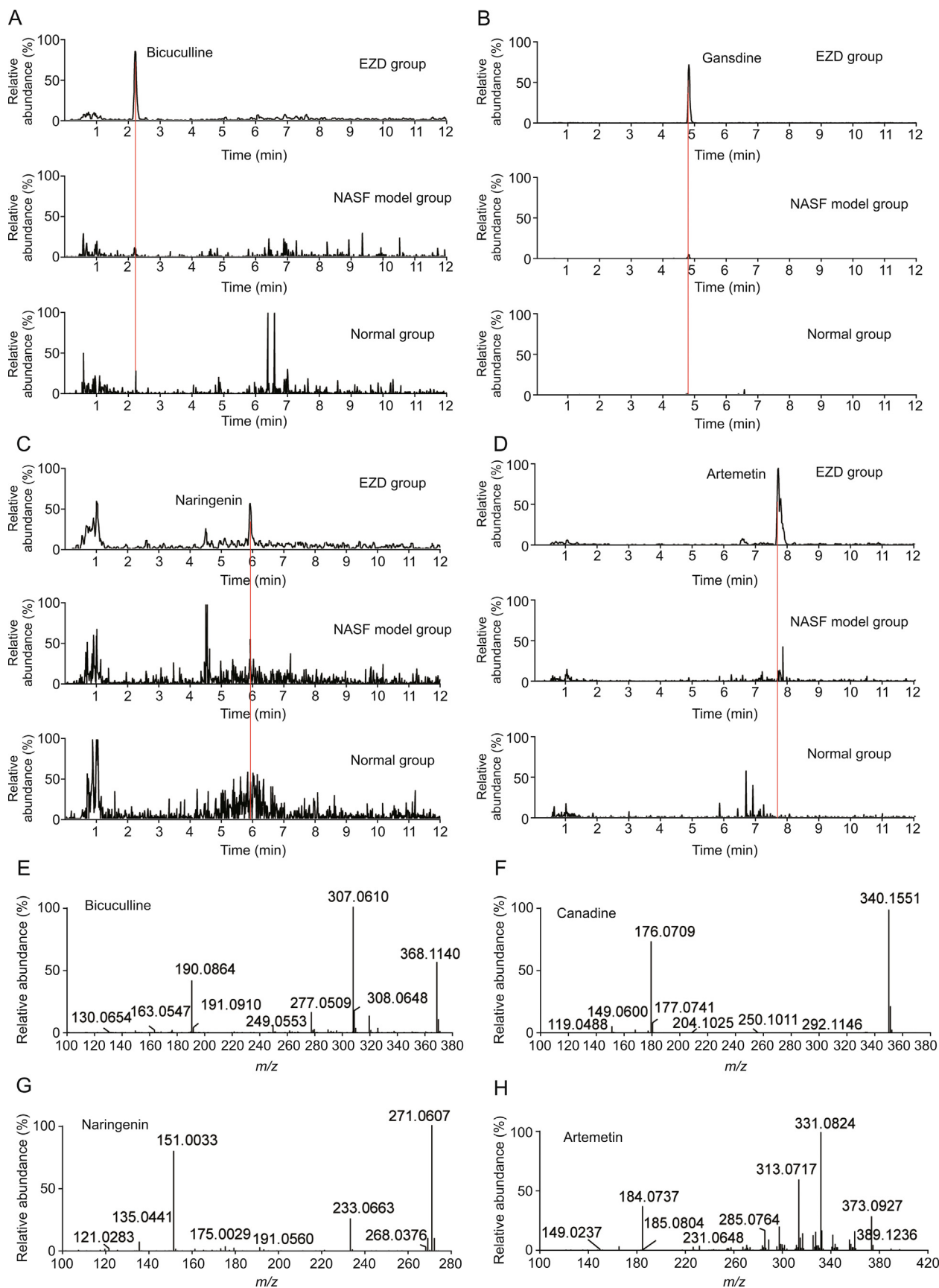


Fig. 5. Extract ion chromatograms of (A) bicuculline, (B) canadine, (C) naringenin, (D) artemetin in the normal, nonalcoholic steatofibrosis (NASF) model and Eight Zhes Decoction (EZD) group. The MS² fragment ion spectra of (E) bicuculline, (F) canadine, (G) naringenin, and (H) artemetin.

Table 2
Four active ingredients detected in liver tissue of mouse administrated of Eight Zhes Decoction (EZD).

| Ingredient | r_t (min) | Experimental m/z | Theoretical m/z | Error (ppm) | Product ions | Formula | Identification |
|------------|-------------|--------------------|-------------------|-------------|-------------------------------------|---|----------------|
| 1 | 2.24 | 368.1138 (+) | 368.1134 | 1.1 | 307.0610,277.0509,190.0864 | C ₂₀ H ₁₇ NO ₆ | Bicuculline |
| 2 | 4.83 | 340.1549 (+) | 340.1549 | 0 | 176.0709 | C ₂₀ H ₂₁ NO ₄ | Canadine |
| 3 | 5.93 | 271.0601 (-) | 271.0606 | 1.8 | 177.0177,151.0022,119.0490 | C ₁₅ H ₁₂ O ₅ | Naringenin |
| 4 | 7.68 | 389.1255 (+) | 389.1236 | 4.9 | 373.0927,331.0824,313.0717,184.0737 | C ₂₀ H ₂₀ O ₈ | Artemetin |

Table 3
Docking information of active ingredients and targets of Eight Zhes Decoction (EZD).

| Term | Binding energy (kcal/mol) | Mode of action | Target point |
|--------------------|---------------------------|----------------|---------------------------|
| PLA2G2A-Naringenin | -7.60 | H bond | LYS-62 |
| CYP3A4-Naringenin | -8.15 | H bond | LYS-476, VAL-490 |
| CYP2C9-Naringenin | -6.29 | H bond | ARG-342, ASN-418 |
| ALOX12-Naringenin | -6.48 | H bond | ILE-318, THR-329 |
| PLA2G2A-Artemetin | -6.50 | H bond | LYS-62, LYS-115 THR-61 |
| CYP2C8-Artemetin | -6.09 | H bond | GLN-214 |
| ALOX12-Artemetin | -5.25 | H bond | CYS-559 |
| CYP3A4-Canadine | -8.63 | H bond | THR-224 |
| CYP1A2-Canadine | -5.97 | H bond | LYS-167 |
| CYP3A4-Bicuculline | -7.46 | H bond | LEU-477 |
| CYP2C9-Bicuculline | -6.91 | H bond | ASN-107, ASN-217 |

accumulation [40]. In addition, PGE2 can promote de novo lipogenesis and accelerate hepatic steatosis [41,42]. Therefore, the limitation of the PGE2 pathway can be considered an effective treatment for NAFLD. EZD was used as a treatment for NAFLD by inhibiting the generation of LTB4 and PGE2, which was found to be upregulated in NASF mice in our study. In addition, 12,13-EpOME and 9,10-EpOME produced by reactions catalyzed by CYP450 were also upregulated in NASF model mice, and their levels were recovered by EZD treatment.

Network pharmacology is widely used to systematically and comprehensively study the effect of drugs on disease based on a “disease-gene-target-drug” network. However, independent online pharmacological studies are highly dependent on public databases and lack data support from actual experiments. Therefore, a strategy integrating lipidomics, network pharmacology and pharmacokinetics was applied. Four ingredients, naringenin, artemetin,

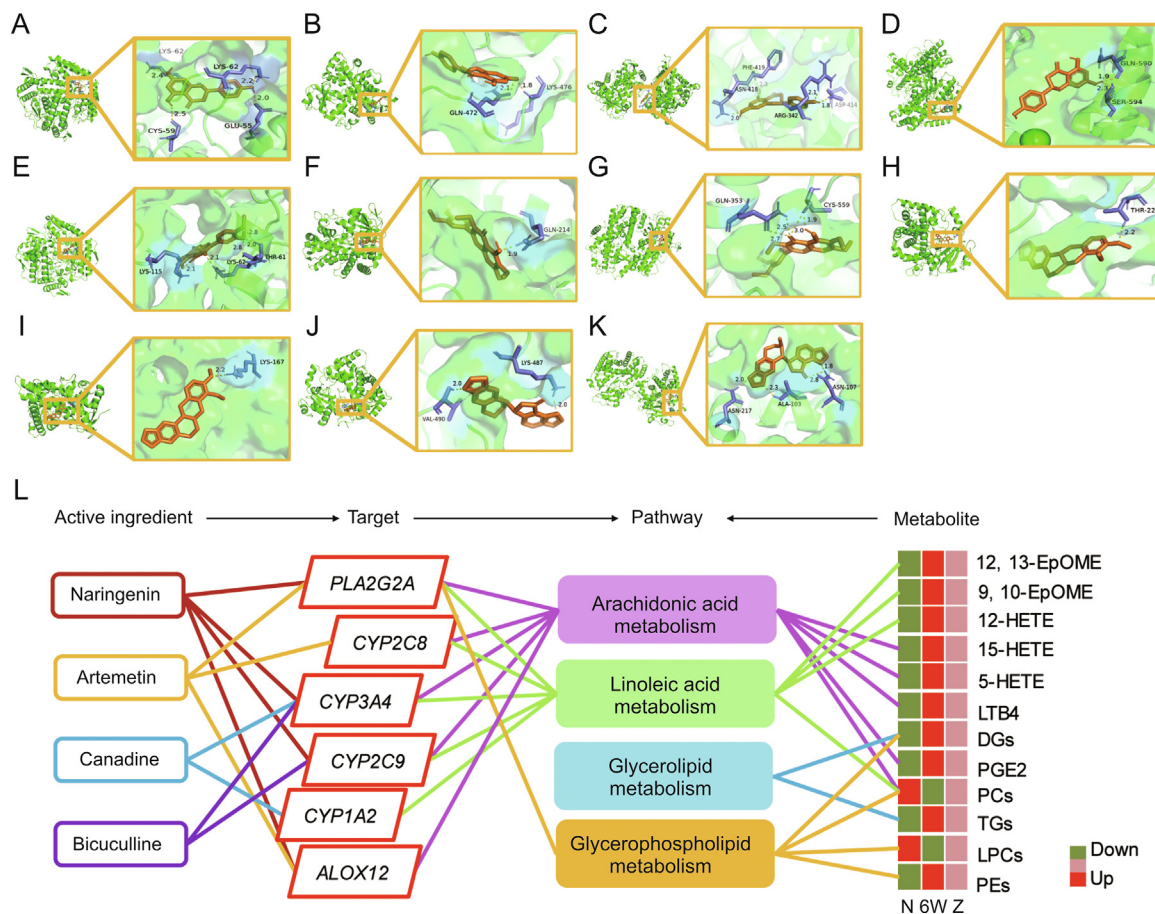


Fig. 6. Molecular docking of the following active ingredients and targets: (A) PLA2G2A-naringenin, (B) CYP3A4-naringenin, (C) CYP2C9-naringenin, (D) ALOX12-naringenin, (E) PLA2G2A-artemetin, (F) CYP2C8-artemetin, (G) ALOX12-artemetin, (H) CYP3A4-canadine, (I) CYP1A2-canadine, (J) CYP3A4-bicuculline, and (K) CYP2C9-bicuculline. (L) Active ingredient-metabolite-target-pathway network of Eight Zhes Decoction (EZD) in nonalcoholic fatty liver disease. EpOME: epoxy-octadecenoic acid; PCs: phosphatidylcholines; DGs: diacylglycerols; HETE: hydroxyeicosatetraenoic acid; TGs: triacylglycerols; LPCs: lysophosphatidylcholines; PGE2: prostaglandin E2; LTB4: leukotriene B4; PEs: phosphatidylethanolamines. N: normal group; 6W: nonalcoholic steatofibrosis (NASF) model group; Z: EZD group.

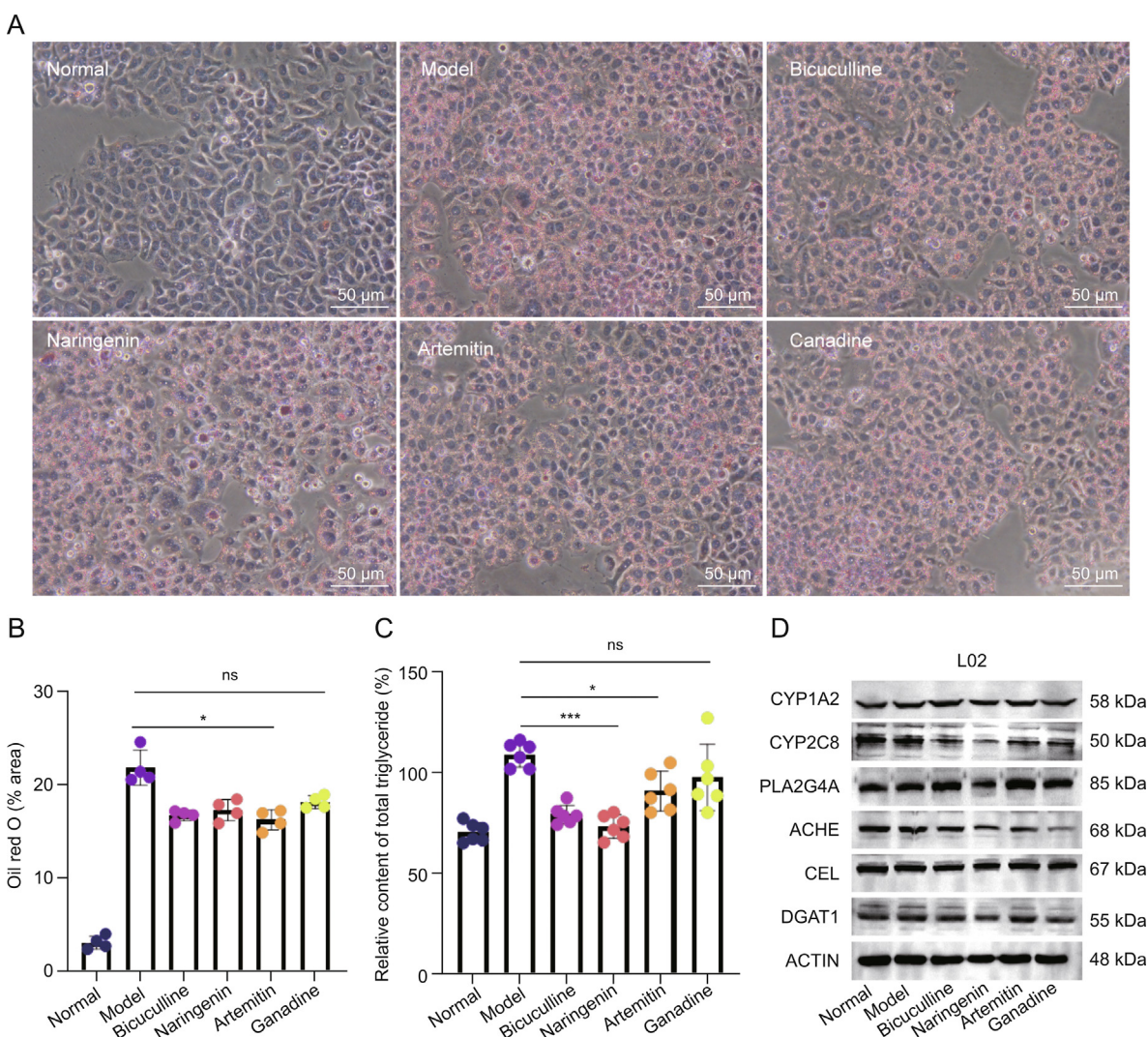


Fig. 7. Validation of the effects of active ingredients and targets. (A) Oil red O staining of L02 cells in the normal, model, bicuculline, naringenin, artemetin, and canadine groups. (B) Lipid droplet area ratio of L02 cell. (C) Relative content of total triacylglycerols of L02 cells. (D) Expression of *CYP1A2*, *CYP2C8*, *PLA2G4A*, *ACHE*, *CEL*, and *DGAT1* proteins in L02 cells belonging to the normal, model, bicuculline, naringenin, artemetin, and canadine groups. * $P < 0.05$ and *** $P < 0.001$ vs. the model group; ns: no significant difference.

canadine, and bicuculline, were identified as the core ingredients against NAFLD, and their corresponding core targets, *PLA2G2A*, *CYP2C8*, *CYP3A4*, *CYP2C9*, *CYP1A2*, and *ALOX12*, were further validated by molecular docking. High affinity among the four ingredients and these targets was observed. In addition, cell experiments based on a high-fat model and western blotting were investigated to verify the four active ingredients and potential targets. Naringenin, artemetin, and bicuculline significantly reversed intracellular TG accumulation in the high-fat model group, and canadine had a similar but nonsignificant effect. Naringenin can reduce the expression levels of *PLA2G4A*, indicating that naringenin could reduce PC consumption by inhibiting the expression of *PLA2G4A* and thus promotes sufficient VLDL synthesis to transport excess TG in the liver. Currently, several clinical trials have investigated naringenin against NAFLD and have demonstrated that naringenin can decrease liver lipid deposition but has no reverse effect on liver injury indices [43,44]. In this study, the chemical ingredients of EZD were considered, but the composition of the decoction is complicated. EZD has many other components, such as carbohydrates, minerals and proteins, which might also have an effect on NAFLD, but this potential effect needs further analysis. In addition, the present study performed a preliminary

investigation of the mechanism, and in-depth studies, such as experiments using knockout mouse to clarify the targets, and studies using clinical sample, are needed.

5. Conclusion

In summary, a strategy integrating lipidomics, network pharmacology and pharmacokinetics was employed to elucidate the active ingredients, targets and pathways of EZD against NAFLD. Glycerophospholipid metabolism, arachidonic acid metabolism, glycerolipid metabolism and linoleic acid metabolism were found to be involved in the treatment effects of EZD, and 12,13-EpOME, PCs, DGs, TGs, LPCs, 9,10-EpOME, 12-HETE, LTB₄, 5-HETE, PGE₂, 15-HETE and PEs were identified as the key metabolites. Importantly, we identified naringenin, artemetin, canadine, and bicuculline as the active compounds of EZD against NAFLD; in particular, naringenin reduces PC consumption by inhibiting the expression of *PLA2G4A* and promotes sufficient VLDL synthesis to transport excess TG in the liver. An in-depth and systematic study is needed to verify the current results. This research provides valuable data and theoretical support for the application of EZD against NAFLD as well as a novel paradigm for elucidating the effective ingredients of

EZD and their potential mechanisms.

CRedit author statement

Yuping Zhou: Conceptualization, Investigation, Resources, Writing - Reviewing and Editing, Funding acquisition; **Ze Dai:** Validation, Investigation, Writing - Reviewing and Editing, Visualization; **Kaili Deng:** Formal analysis, Investigation, Visualization; **Yubin Wang:** Software, Investigation, Visualization; **Jiaming Ying, Donghui Chu,** and **Jinyue Zhou:** Investigation; **Chunlan Tang:** Conceptualization, Methodology, Resources, Writing - Original draft preparation, Reviewing and Editing, Visualization, Supervision, Funding acquisition.

Declaration of competing interest

The authors declare that there are no conflicts of interest.

Acknowledgments

This work was supported by Ningbo Natural Science Foundation (Grant No.: 2022J229), Project of Ningbo Leading Medical & Health Discipline (Project No.: 2022–S04), Opened-end Fund of Key Laboratory (Grant No.: KFJJ-202101), and Graduate Student Scientific Research and Innovation Fund of Ningbo University (Grant No.: IF2022193).

Appendix A. Supplementary data

Supplementary data to this article can be found online at <https://doi.org/10.1016/j.jpha.2023.05.012>.

References

- [1] E. Bugianesi, S. Petta, NAFLD/NASH, *J. Hepatol.* 77 (2022) 549–550.
- [2] M.H. Le, Y.H. Yeo, X. Li, et al., 2019 global NAFLD prevalence: A systematic review and meta-analysis, *Clin. Gastroenterol. Hepatol.* 20 (2022) 2809–2817.e28.
- [3] S.L. Friedman, B.A. Neuschwander-Tetri, M. Rinella, et al., Mechanisms of NAFLD development and therapeutic strategies, *Nat. Med.* 24 (2018) 908–922.
- [4] C. Alonso, D. Fernández-Ramos, M. Varela-Rey, et al., Metabolomic identification of subtypes of nonalcoholic steatohepatitis, *Gastroenterology* 152 (2017) 1449–1461.e7.
- [5] R.J. Perry, V.T. Samuel, K.F. Petersen, et al., The role of hepatic lipids in hepatic insulin resistance and type 2 diabetes, *Nature* 510 (2014) 84–91.
- [6] P.K. Luukkonen, Y. Zhou, S. Sädevirta, et al., Hepatic ceramides dissociate steatosis and insulin resistance in patients with non-alcoholic fatty liver disease, *J. Hepatol.* 64 (2016) 1167–1175.
- [7] M.S. Han, S.Y. Park, K. Shinzawa, et al., Lysophosphatidylcholine as a death effector in the lipoapoptosis of hepatocytes, *J. Lipid Res.* 49 (2008) 84–97.
- [8] A. Krishnan, T.S. Abdullah, T. Mounajjed, et al., A longitudinal study of whole body, tissue, and cellular physiology in a mouse model of fibrosing NASH with high fidelity to the human condition, *Am. J. Physiol. Gastrointest. Liver Physiol.* 312 (2017) G666–G680.
- [9] E. Vilar-Gomez, Y. Martinez-Perez, L. Calzadilla-Bertot, et al., Weight loss through lifestyle modification significantly reduces features of nonalcoholic steatohepatitis, *Gastroenterology* 149 (2015) 367–378.e5.
- [10] R. Xu, J. Pan, W. Zhou, et al., Recent advances in lean NAFLD, *Biomed. Pharmacother.* 153 (2022), 113331.
- [11] F. Chen, S. Esmaili, G. B. Rogers, et al., Lean NAFLD: A distinct entity shaped by differential metabolic adaptation, *Hepatology* 71 (2020) 1213–1227.
- [12] M. Shao, Y. Lu, H. Xiang, et al., Application of metabolomics in the diagnosis of non-alcoholic fatty liver disease and the treatment of traditional Chinese medicine, *Front. Pharmacol.* 13 (2022), 971561.
- [13] Y. Deng, M. Pan, H. Nie, et al., Lipidomic analysis of the protective effects of Shenling Baizhu San on non-alcoholic fatty liver disease in rats, *Molecules* 24 (2019), 3943.
- [14] S.-H. Park, J.-E. Lee, S.M. Lee, et al., An unbiased lipidomics approach identifies key lipid molecules as potential therapeutic targets of Dohongsamul-tang against non-alcoholic fatty liver diseases in a mouse model of obesity, *J. Ethnopharmacol.* 260 (2020), 112999.
- [15] Y. Zhou, J. Yang, P. Yang, et al., Prospective cohort study of “Eight Zhes” Decoction in the treatment of non-alcoholic steatohepatitis, *Chin. J. Mod. Appl. Pharm.* 36 (2019) 2197–2201.
- [16] J. Ru, P. Li, J. Wang, et al., TCMSIP: A database of systems pharmacology for drug discovery from herbal medicines, *J. Cheminform.* 6 (2014), 13.
- [17] D. Szklarczyk, A. Santos, C. von Mering, et al., STITCH 5: Augmenting protein-chemical interaction networks with tissue and affinity data, *Nucleic Acids Res.* 44 (2016) D380–D384.
- [18] D. Gfeller, O. Michielin, V. Zoete, Shaping the interaction landscape of bioactive molecules, *Bioinformatics* 29 (2013) 3073–3079.
- [19] X. Wang, Y. Shen, S. Wang, et al., PharmMapper 2017 update: A web server for potential drug target identification with a comprehensive target pharmacophore database, *Nucleic Acids Res.* 45 (2017) W356–W360.
- [20] M. J. Keiser, B. L. Roth, B.N. Armbruster, et al., Relating protein pharmacology by ligand chemistry, *Nat. Biotechnol.* 25 (2007) 197–206.
- [21] G. Stelzel, N. Rosen, I. Plaschkes, et al., The geneCards suite: From gene data mining to disease genome sequence analyses, *Curr. Protoc. Bioinformatics* 54 (2016) 1.30.1–1.30.33.
- [22] D.W. Huang, B. T. Sherman, R.A. Lempicki, Systematic and integrative analysis of large gene lists using DAVID bioinformatics resources, *Nat. Protoc.* 4 (2009) 44–57.
- [23] P. Shannon, A. Markiel, O. Ozier, et al., Cytoscape: A software environment for integrated models of biomolecular interaction networks, *Genome Res.* 13 (2003) 2498–2504.
- [24] H.M. Berman, J. Westbrook, Z. Feng, et al., The protein data bank, *Nucleic Acids Res.* 28 (2000) 235–242.
- [25] S. Kim, J. Chen, T. Cheng, et al., PubChem 2023 update, *Nucleic Acids Res.* 51 (2023) D1373–D1380.
- [26] D.S. Goodsell, A.J. Olson, Automated docking of substrates to proteins by simulated annealing, *Proteins* 8 (1990) 195–202.
- [27] C.A. Schneider, W.S. Rasband, K.W. Eliceiri, NIH Image to ImageJ: 25 years of image analysis, *Nat. Methods* 9 (2012) 671–675.
- [28] Y. Zhang, J. Lv, J. Zhang, et al., Lipidomic-based investigation into the therapeutic effects of polyene phosphatidylcholine and Babao Dan on rats with non-alcoholic fatty liver disease, *Biomed. Chromatogr.* 36 (2022), e5271.
- [29] X. Li, J. Ge, Y. Li, et al., Integrative lipidomic and transcriptomic study unravels the therapeutic effects of saikosaponins A and D on non-alcoholic fatty liver disease, *Acta Pharm. Sin. B* 11 (2021) 3527–3541.
- [30] H. Liu, T. Chen, X. Xie, et al., Hepatic lipidomics analysis reveals the ameliorative effects of highland barley β -glucan on western diet-induced nonalcoholic fatty liver disease mice, *J. Agric. Food Chem.* 69 (2021) 9287–9298.
- [31] A. Kotronen, V.R. Velagapudi, L. Yetukuri, et al., Serum saturated fatty acids containing triacylglycerols are better markers of insulin resistance than total serum triacylglycerol concentrations, *Diabetologia* 52 (2009) 684–690.
- [32] D.L. Gorden, D.S. Myers, P.T. Ivanova, et al., Biomarkers of NAFLD progression: A lipidomics approach to an epidemic, *J. Lipid Res.* 56 (2015) 722–736.
- [33] R. Mayo, J. Crespo, I. Martínez-Arranz, et al., Metabolomic-based noninvasive serum test to diagnose nonalcoholic steatohepatitis: Results from discovery and validation cohorts, *Hepatol. Commun.* 2 (2018) 807–820.
- [34] F. Bril, L. Millán, S. Kalavalapalli, et al., Use of a metabolomic approach to non-invasively diagnose non-alcoholic fatty liver disease in patients with type 2 diabetes mellitus, *Diabetes Obes. Metab.* 20 (2018) 1702–1709.
- [35] J. Simon, M. Nuñez-García, P. Fernández-Tussy, et al., Targeting hepatic glutaminase 1 ameliorates non-alcoholic steatohepatitis by restoring very-low-density lipoprotein triglyceride assembly, *Cell Metab.* 31 (2020) 605–622.e10.
- [36] P. Puri, R.A. Baillie, M.M. Wiest, et al., A lipidomic analysis of nonalcoholic fatty liver disease, *Hepatology* 46 (2007) 1081–1090.
- [37] J. Barr, J. Caballería, I. Martínez-Arranz, et al., Obesity-dependent metabolic signatures associated with nonalcoholic fatty liver disease progression, *J. Proteome Res.* 11 (2012) 2521–2532.
- [38] Z. Gai, M. Visentin, T. Gui, et al., Effects of farnesoid X receptor activation on arachidonic acid metabolism, NF- κ B signaling, and hepatic inflammation, *Mol. Pharmacol.* 94 (2018) 802–811.
- [39] X. Liu, K. Wang, L. Wang, et al., Hepatocyte leukotriene B4 receptor 1 promotes NAFLD development in obesity, *Hepatology* (2022). <https://doi.org/10.1002/hep.32708>.
- [40] W. Wang, X. Zhong, J. Guo, Role of 2-series prostaglandins in the pathogenesis of type 2 diabetes mellitus and non-alcoholic fatty liver disease (Review), *Int. J. Mol. Med.* 47 (2021), 114.
- [41] J. Henkel, K. Frede, N. Schanze, et al., Stimulation of fat accumulation in hepatocytes by PGE $_2$ -dependent repression of hepatic lipolysis, β -oxidation and VLDL-synthesis, *Lab. Invest.* 92 (2012) 1597–1606.
- [42] M.-Y. Chung, E. Mah, C. Masterjohn, et al., Green tea lowers hepatic COX-2 and prostaglandin E2 in rats with dietary fat-induced nonalcoholic steatohepatitis, *J. Med. Food* 18 (2015) 648–655.
- [43] Z. Namkhah, F. Naeini, S. Mahdi Rezayat, et al., Does naringenin supplementation improve lipid profile, severity of hepatic steatosis and probability of liver fibrosis in overweight/obese patients with NAFLD? A randomised, double-blind, placebo-controlled, clinical trial, *Int. J. Clin. Pract.* 75 (2021), e14852.
- [44] F. Naeini, Z. Namkhah, H. Tutunchi, et al., Effects of naringenin supplementation in overweight/obese patients with non-alcoholic fatty liver disease: Study protocol for a randomized double-blind clinical trial, *Trials* 22 (2021), 801.